The Astrophysical Journal, 782:93 (12pp), 2014 February 20 doi:10.1088/0004-637X/782/2/93

IS A DEEP ONE-CELL MERIDIONAL CIRCULATION ESSENTIAL FOR THE FLUX TRANSPORT SOLAR DYNAMO?

Gopal Hazra[1,2], Bidya Binay Karak[1,3], and Arnab Rai Choudhuri[1]
[1] Department of Physics, Indian Institute of Science, Bangalore 560012, India; ghazra@physics.iisc.ernet.in
[2] Indian Institute of Astrophysics, Bangalore 560034, India
[3] Nordita KTH Royal Institute of Technology and Stockholm University, Roslagstullsbacken 23, SE-106 91 Stockholm, Sweden
Received 2013 September 10; accepted 2013 December 17; published 2014 February 3

ABSTRACT

The solar activity cycle is successfully modeled by the flux transport dynamo, in which the meridional circulation of the Sun plays an important role. Most of the kinematic dynamo simulations assume a one-cell structure of the meridional circulation within the convection zone, with the equatorward return flow at its bottom. In view of the recent claims that the return flow occurs at a much shallower depth, we explore whether a meridional circulation with such a shallow return flow can still retain the attractive features of the flux transport dynamo (such as a proper butterfly diagram, the proper phase relation between the toroidal and poloidal fields). We consider additional cells of the meridional circulation below the shallow return flow—both the case of multiple cells radially stacked above one another and the case of more complicated cell patterns. As long as there is an equatorward flow in low latitudes at the bottom of the convection zone, we find that the solar behavior is approximately reproduced. However, if there is either no flow or a poleward flow at the bottom of the convection zone, then we cannot reproduce solar behavior. On making the turbulent diffusivity low, we still find periodic behavior, although the period of the cycle becomes unrealistically large. In addition, with a low diffusivity, we do not get the observed correlation between the polar field at the sunspot minimum and the strength of the next cycle, which is reproduced when diffusivity is high. On introducing radially downward pumping, we get a more reasonable period and more solar-like behavior even with low diffusivity.

Key words: dynamo – Sun: activity – Sun: magnetic fields

Online-only material: color figures

1. INTRODUCTION

The most extensively studied theoretical model of the solar activity cycle in the last few years is the flux transport dynamo model, originally proposed in the 1990s (Wang et al. 1991; Choudhuri et al. 1995; Durney 1995) and recently reviewed by several authors (Charbonneau 2010; Choudhuri 2011). This model had remarkable success in explaining various aspects of the solar cycle and its irregularities. However, in spite of its success, doubts are often expressed if this success is merely accidental or if this is the really correct model. Essentially, the answer hinges on whether the various assumptions used in the model are correct.

Let us consider the crucial assumptions of the model. The toroidal magnetic field is assumed to be produced from the poloidal field by the differential rotation that is mapped by helioseismology, leaving no scope for any doubts. This toroidal field rises due to magnetic buoyancy to the solar surface, where the poloidal magnetic field is produced from it by the Babcock–Leighton mechanism (Babcock 1961; Leighton 1964), for which there is now strong observational support (Dasi-Espuig et al. 2010; Kitchatinov & Olemskoy 2011a; Muñoz-Jaramillo et al. 2013). Magnetic buoyancy and the Babcock–Leighton mechanism are inherently three-dimensional processes and their representation in a two-dimensional kinematic model can never be fully realistic (Muñoz-Jaramillo et al. 2010; Yeates & Muñoz-Jaramillo 2013). There are also considerable uncertainties in the values of some parameters, such as the turbulent diffusivity inside the convection zone. The Boulder group (Dikpati et al. 2004) and the Bangalore group (Chatterjee et al. 2004) used values of turbulent diffusivity that differ by a factor of about 50. The higher diffusivity used by the Bangalore group now has strong support due to its success in explaining various aspects of the observational data (Chatterjee et al. 2004; Chatterjee & Choudhuri 2006; Jiang et al. 2007; Goel & Choudhuri 2009; Hotta & Yokoyama 2010; Karak 2010; Karak & Choudhuri 2011, 2012, 2013; Choudhuri & Karak 2009, 2012; Miesch et al. 2012; Muñoz-Jaramillo et al. 2013). Because of these uncertainties in the treatment of the Babcock–Leighton mechanism and in the value of turbulent diffusivity, it is necessary to interpret the results of the flux transport dynamo model with some degree of caution. However, these uncertainties do not invalidate the model. After all, different treatments of the Babcock–Leighton mechanism and a range of values for the turbulent diffusivity seem to give qualitatively similar results. The only other important ingredient of the flux transport dynamo model is the meridional circulation. Because the nature of the meridional circulation in the deeper layers of the convection zone is not yet observationally established, the main source of doubt about the flux transport dynamo model at the present time concerns the question of whether the Sun has the kind of meridional circulation that is assumed in the flux transport dynamo models.

Let us consider the role of the meridional circulation in flux transport dynamo models. In order for sunspots to form at lower and lower latitudes with the progress of the cycle, a condition known as the Parker–Yoshimura sign rule was expected to be satisfied (Parker 1955; Yoshimura 1975; see also Choudhuri 1998, Section 16.6). According to this condition, $\alpha\,\partial\Omega/\partial r$ has to be negative in the northern hemisphere. It follows from observations of the solar surface that α corresponding to the Babcock–Leighton mechanism is positive in the northern hemisphere. Helioseismology shows that $\partial\Omega/\partial r$ is also positive in the lower latitudes where sunspots are seen (except in

a shear layer just below the solar surface). So, clearly the Parker–Yoshimura sign rule is not satisfied and it may be expected that the dynamo wave will propagate in the poleward direction, contrary to observations. Choudhuri et al. (1995) showed that an equatorward meridional circulation at the bottom of the convection zone can overcome the Parker–Yoshimura sign rule and make the dynamo wave propagate in the correct direction. This is the main role of the meridional circulation in the flux transport dynamo models. The second role of the meridional circulation is that the poleward meridional circulation near the solar surface advects the poloidal field poleward, as seen in the observations. In dynamo models with low turbulent diffusivity, the meridional circulation has a third important role. It brings the poloidal field created near the surface to the bottom of the convection zone where the strong differential rotation can act on it to create the toroidal field. In dynamo models with high turbulent diffusivity, however, the poloidal field can diffuse from the surface to the bottom of the convection zone (typically, in about 5 yr) and this third role of the meridional circulation is redundant (Jiang et al. 2007). If there is radial pumping, as suggested by some authors (Karak & Nandy 2012), then that further eliminates the role of meridional circulation for bringing the poloidal field to the bottom of the convection zone. Because we will be using a higher value of turbulent diffusivity in many of our calculations, the twin roles of the meridional circulation in our model will be the equatorward advection of the toroidal field at the bottom of the convection zone and the poleward advection of the poloidal field near the surface.

The simplest kind of meridional circulation assumed in most theoretical models consists of one cell encompassing a hemisphere of the convection zone, with a poleward flow in the upper layers and an equatorward flow in the lower layers. This kind of meridional circulation successfully plays the twin roles expected of it in a flux transport dynamo model. Observations show a poleward meridional circulation near the surface, so there is absolutely no doubt that this part of the meridional circulation advects the poloidal field poleward. The only remaining question is whether the cell of the meridional circulation really penetrates to the bottom of the convection zone where the equatorward flow branch has to be located for the equatorward advection of the toroidal field. Early helioseismic investigations going to a depth of 0.85 $R_\odot$ could not find any evidence of the equatorward return flow until that depth (Giles et al. 1997; Braun & Fan 1998). However, recently, Hathaway (2012), assuming that the supergranules are advected by the meridional circulation, analyzed observational data to conclude that the return flow occurs at depths as shallow as 50–70 Mm. Zhao et al. (2013) also claim, on the basis of their helioseismic inversion, that the equatorward return flow exists between radii 0.82 $R_\odot$ and 0.91 $R_\odot$. On the other hand, Schad et al. (2013), from the study of global helioseismic analysis, find the indication of multi-cell meridional circulation in the whole convection zone. If these results are supported by other independent groups and turn out to be true, then the important question is whether the attractive aspects of the present flux transport dynamo models can be retained with such a meridional circulation. In this paper, we explore whether additional cells of meridional circulation below the shallow return flow can help us solve the problem.

So far, only a few theoretical studies of the flux transport dynamo with a meridional circulation more complicated than a single cell have been carried out. The effects of two cells in the latitudinal direction have been considered by Dikpati et al. (2004) and Bonanno et al. (2005). However, we now want to consider a more complicated structure of the meridional circulation in the radial direction, including the possibility of multiple cells in the radial direction. Such a study was first carried out by Jouve & Brun (2007). In their calculations, they always had poleward meridional circulation at the bottom of the convection zone in the lower latitudes where sunspots are seen. They were able to obtain periodic solutions, but the butterfly diagrams were always in the wrong sense, implying poleward migration of the toroidal field. They concluded that "the resulting butterfly diagram and phase relationship between the toroidal and poloidal fields are affected to a point where it is unlikely that such multicellular meridional flows persist for a long period of time inside the Sun, without having to reconsider the model itself" (Jouve & Brun 2007, p. 239). If this conclusion were generally true for any meridional circulation more complicated than the simple, single-cell circulation, then the results of Hathaway (2012), Schad et al. (2013), and Zhao et al. (2013), if supported by independent investigations by other groups, would indeed be bad news for flux transport dynamo models. Guerrero & de Gouveia Dal Pino (2008) considered a single cell confined to the upper layers of the convection zone. On introducing strong radial and latitudinal pumping, they were able to obtain correct butterfly diagrams. However, whether such equatorward latitudinal pumping actually exists is highly questionable. Another recent attempt to save the flux transport dynamo was made by Pipin & Kosovichev (2013), who used the near-surface shear layer found in helioseismology and an equatorward return flow of meridional circulation just below it. Because $\partial\Omega/\partial r$ is negative within this shear layer, such a dynamo would have equatorward propagation, according to the Parker–Yoshimura sign rule, even in the absence of an equatorward meridional circulation in the right place. However, we are unable to accept the model from Pipin & Kosovichev (2013) as a satisfactory model of the solar cycle for the following reasons. Magnetic buoyancy is particularly destabilizing in the upper layers of the convection zone and it is impossible to store magnetic fields generated there for sufficient time for dynamo amplification (Parker 1975; Moreno-Insertis 1983). Also, the scenario that the toroidal field is generated within the tachocline and then parts of it rise to produce active regions can explain many aspects of active regions, including Joy's law, rather elegantly (Choudhuri 1989; D'Silva & Choudhuri 1993; Fan et al. 1993; Caligari et al. 1995). We find no compelling reason to discard the scenario that the toroidal magnetic field is produced in the tachocline, where magnetic buoyancy is suppressed in the regions of sub-adiabatic temperature gradient (Moreno-Insertis et al. 1992).

The main aim of the present paper is to address the question of whether a meridional circulation with a return flow at a relatively shallow depth would allow us to retain the attractive features of the flux transport dynamo, without introducing such uncertain assumptions as strong equatorward pumping and without abandoning the scenario in which the toroidal field is generated and stored in the tachocline from where it rises to produce active regions. If there is a return flow at a shallow depth and there are no flows underneath it, then we find that the solar cycle cannot be modeled properly with such a flow. However, if there are additional cells of meridional circulation below the shallow return flow, we find that we can retain most of the attractive features of the flux transport dynamo model, as long as there is a layer of equatorward flow in low latitudes at the bottom of the convection zone. The existence of such an equatorward

flow at the bottom of the convection zone is consistent with the findings of Zhao et al. (2013), who were unable to extend their inversion below 0.75 $R_\odot$ using their limited data set. Because our knowledge of the meridional circulation, either from observational or theoretical considerations, is very limited, in this paper, we take the meridional circulation as a free parameter that can be assumed to have any form involving multiple cells, and explore the dynamo problem with different kinds of meridional circulation.

We discuss the mathematical formulation of our dynamo model in Section 2. In Section 3 we present our results for several cells of meridional circulation in the radial direction, while Section 4 presents results for more complicated meridional circulation with multiple cells in both radial and latitudinal directions. Whether or not the results are modified for low turbulent diffusivity will be discussed in Section 5. The effect of turbulent pumping will be discussed in Section 6. Finally, we summarize our conclusions in Section 7.

2. MATHEMATICAL FORMULATION

In the two-dimensional kinematic flux transport dynamo model, we represent the magnetic field as

$$\mathbf{B} = B\hat{\mathbf{e}}_\phi + \nabla \times (A\hat{\mathbf{e}}_\phi), \tag{1}$$

where $B(r,\theta)$ and $A(r,\theta)$ correspond to the toroidal and poloidal components, respectively, which satisfy the following equations:

$$\frac{\partial A}{\partial t} + \frac{1}{s}(\mathbf{v}.\nabla)(sA) = \eta_p\left(\nabla^2 - \frac{1}{s^2}\right)A + S(r,\theta,t), \tag{2}$$

$$\frac{\partial B}{\partial t} + \frac{1}{r}\left[\frac{\partial}{\partial r}(rv_rB) + \frac{\partial}{\partial\theta}(v_\theta B)\right] = \eta_t\left(\nabla^2 - \frac{1}{s^2}\right)B + s(\mathbf{B}_p\ .\ \nabla)\Omega + \frac{1}{r}\frac{d\eta_t}{dr}\frac{\partial(rB)}{\partial r}, \tag{3}$$

where $s = r\sin\theta$. Here $\mathbf{v}$ is velocity of the meridional flow, Ω is the internal angular velocity of the Sun, η_p and η_t are turbulent diffusivities, and $S(r,\theta,t)$ is the coefficient that describes the generation of the poloidal field at the solar surface from the decay of bipolar sunspots. These equations have to be solved with the boundary conditions $A = B = 0$ at $\theta = 0, \pi$, whereas at the top boundary, $B = 0$ and A, matches a potential field above (Dikpati & Choudhuri 1995). The bottom boundary condition does not affect the solutions as long as the bottom of the integration region is taken sufficiently below the bottom of the convection zone. Once the parameters Ω, η_p, η_t, $\mathbf{v}$, and $S(r,\theta,t)$ are specified, Equations (2) and (3) can be solved with the code *Surya* to obtain the behavior of the dynamo (Nandy & Choudhuri 2002; Chatterjee et al. 2004). Chatterjee et al. (2004) present a detailed discussion of how the parameters were specified in their simulations. However, Karak (2010) made some small changes in the parameters. In the calculations in this paper, we use Ω, η_p, and η_t as Karak (2010), except that Sections 5 and 6 present some discussion with different diffusivities, which will be explained in Section 5. In this paper, we carry out dynamo simulations with different kinds of meridional circulation $\mathbf{v}$. Before coming to the meridional circulation, we will describe how we specified the poloidal source term $S(r,\theta,t)$.

The effects of the magnetic buoyancy and the Babcock–Leighton mechanism have to be incorporated by suitably specifying the poloidal source term $S(r,\theta,t)$. There are two widely used procedures to specify magnetic buoyancy. In the first procedure, whenever the toroidal field B at the bottom of the convection zone crosses a critical value, a part of it is brought to the solar surface. In the second procedure, the Babcock–Leighton coefficient α in the source term multiplies the toroidal magnetic field at the bottom of the convection zone rather than the local toroidal field. Although the two procedures do not give identical results, even with all the other parameters kept the same (Choudhuri et al. 2005), they both reproduce the qualitative behaviors of the solar cycle. Because we believe that the first procedure is more realistic, we used it in the majority of calculations from our group (Chatterjee et al. 2004; Choudhuri et al. 2007; Karak 2010). However, it can be difficult to introduce this procedure in a stable way when the meridional circulation is made very complicated. Because we are studying the behavior of the dynamo with various complicated meridional circulations, we opted for the second procedure. We specify the poloidal source term in Equation (2) in the following way:

$$S(r,\theta;\,B) = \frac{\alpha(r,\theta)}{1 + (\overline{B}(r_t,\theta)/B_0)^2}\overline{B}(r_t,\theta), \tag{4}$$

where $\overline{B}(r_t,\theta)$ is the value of the toroidal field at latitude θ averaged over the tachocline from $r = 0.685\ R_\odot$ to $r = 0.715\ R_\odot$. We take

$$\alpha(r,\theta) = \frac{\alpha_0}{4}\left[1 + \mathrm{erf}\left(\frac{r - 0.95\ R_\odot}{0.05\ R_\odot}\right)\right]\left[1 - \mathrm{erf}\left(\frac{r - R_\odot}{0.01\ R_\odot}\right)\right] \times \sin\theta\cos\theta\left[\frac{1}{1 + e^{-30(\theta - \pi/4)}}\right]. \tag{5}$$

Note that the last factor in Equation (5) suppresses α in the higher latitudes and constrains the butterfly diagram from extending to very high latitudes. We are following many previous authors who also suppressed α in high latitudes by such means (Muñoz-Jaramillo et al. 2010; Hotta & Yokoyama 2010). Because the suppression of α is not based on a clear physical reason, we did not use the suppression of α in the previous calculations from our group using the first procedure of treating magnetic buoyancy outlined above. However, when treating magnetic buoyancy by the second procedure, flux eruptions tend to occur at higher latitudes (Choudhuri et al. 2005) and it becomes necessary to suppress eruptions at high latitudes to get more reasonable butterfly diagrams. For the calculations presented in Sections 3 and 4 using high diffusivity, we use $\alpha_0 = 8.0$ m s^{-1}. In the low diffusivity case presented in Section 5, we use a lower value $\alpha_0 = 0.5$ m s^{-1}. When we include the effect of radial turbulent pumping in Section 6 we use $\alpha_0 = 0.1$ m s^{-1}. Note that the parameter B_0 in Equation (4) introduces the only nonlinearity in the problem and determines the amplitude of the magnetic field. We will later present magnetic fields in units of B_0.

Below we discuss how the meridional circulation is prescribed. The meridional circulation is always defined in terms of stream function ψ, which is given by

$$\rho\mathbf{v} = \nabla \times [\psi(r,\theta)\mathbf{e}_\phi], \tag{6}$$

with the density profile given by

$$\rho = C\left(\frac{R_\odot}{r} - 0.95\right)^{3/2}, \tag{7}$$

We can generate different types of meridional circulation by choosing ψ suitably. For example, the one-cell meridional

circulation used in many of the recent works from our group (Karak 2010) is obtained by taking

$$\psi r \sin\theta = \psi_0 (r - R_p) \sin\left[\frac{\pi (r - R_p)}{(R_\odot - R_p)}\right] \{1 - e^{-\beta_1 \theta^\epsilon}\} \times \{1 - e^{\beta_2 (\theta - \pi/2)}\} e^{-((r-r_0)/\Gamma)^2}, \quad (8)$$

with $\beta_1 = 1.5$, $\beta_2 = 1.3$, $\epsilon = 2.0000001$, $r_0 = (R_\odot - R_b)/3.5$, $\Gamma = 3.47 \times 10^8$ m, $R_p = 0.635\ R_\odot$. The value of ψ_0/C determines the amplitude of the meridional circulation. On taking $\psi_0/C = 0.95 \times 15.0$, the poleward flow near the surface at mid-latitudes peaks around $v_0 = 15.0$ m s^{-1}. The cell of the meridional circulation is confined between R_p and $R_\odot$. By making R_p larger (but less than $R_\odot$), we can make the meridional circulation confined in the upper layers of the convection zone.

In order to have N cells of meridional circulation, we can take a stream function of the form

$$\psi = \psi_1 + \psi_2 + \cdots + \psi_N, \quad (9)$$

where each term in the stream function gives rise to a cell of meridional circulation. Here we describe how we generate a two-cell meridional circulation pattern, which is used in some of our simulations. The details of how we generate three-cell and more complicated patterns are given in the Appendix. Because Zhao et al. (2013) claim that the upper cell of the meridional circulation is confined above 0.82 $R_\odot$, we did some calculations with two cells above and below $R_m = 0.82\ R_\odot$. To generate such a pattern of meridional circulation, we used the stream function

$$\psi = \psi_u + \psi_l. \quad (10)$$

The stream function ψ_u, which generates the upper cell, is given by

$$\psi_u = \psi_{0u}\left[1 - \mathrm{erf}\left(\frac{r - 0.91\ R_\odot}{1.0}\right)\right](r - R_{m,u}) \times \sin\left[\frac{\pi (r - R_{m,u})}{(R_\odot - R_{m,u})}\right]\{1 - e^{-\beta_1 \theta^\epsilon}\} \times \{1 - e^{\beta_2 (\theta - \pi/2)}\} e^{-((r-r_0)/\Gamma)^2}, \quad (11)$$

where the parameters have the following values: $\beta_1 = 3.5$, $\beta_2 = 3.3$, $r_0 = (R_\odot - R_b)/3.5$, $\Gamma = 3.4 \times 10^8$ m, $R_{m,u} = 0.815\ R_\odot$. The stream function ψ_l, which generates the lower cell, is given by

$$\psi_l = \psi_{0l}\left[1 - \mathrm{erf}\left(\frac{r - 0.95 R_{m,l}}{1.8}\right)\right](r - R_p) \times \sin\left[\frac{\pi (r - R_p)}{(R_{m,l} - R_p)}\right]\{1 - e^{-\beta_1 \theta^\epsilon}\} \times \{1 - e^{\beta_2 (\theta - \pi/2)}\} e^{-((r-r_0)/\Gamma)^2}, \quad (12)$$

where the parameters have the following values: $\beta_1 = 3.2$, $\beta_2 = 3.0$, $r_0 = (R_\odot - R_b)/3.5$, $\Gamma = 3.24 \times 10^8$ m, $R_p = 0.65\ R_\odot$, $R_{m,l} = 0.825\ R_\odot$. We chose ψ_{0u}/C and ψ_{0l}/C in such a way that the velocity amplitudes in the upper and lower cells were around 20.0 m s^{-1} and 4.0 m s^{-1}, respectively.

The two-cell meridional circulation given by the above expressions is shown in the upper part of Figure 2. Figure 2(a) shows the streamlines of flow and Figure 2(b) shows how v_θ varies with r at the mid-latitude. The vertical dashed lines in Figure 2(b) indicate the bottoms and tops of the two cells. Note that both the cells have counter-clockwise flow patterns, which means that the flows at the bottom of the upper cell and at the top of the lower cell (which are adjacent to each other) are in opposite directions, involving a jump in the value of v_θ from one cell to the next, as seen in Figure 2(b). If we replace ψ_l by $-\psi_l$, then we can avoid this jump in the value of v_θ. This flow pattern is shown in the upper part of Figure 3, however, the meridional circulation at the tachocline is in the poleward direction. Section 3 will show that this case will not give solar-like solutions. If we want the meridional circulation to be poleward at the surface and equatorward at the tachocline, and additionally we want to avoid a jump in v_θ, then we need at least three cells stacked one above the other in the radial direction. The flows in the top and bottom cells have to be counter-clockwise, whereas the flow in the middle cell has to be clockwise. The Appendix presents the steam function that would give this flow, which is shown in the upper part of Figure 4. The results from all the flow patterns are presented in the next section and results from the more complicated flow will be presented in Section 4. When we discuss the effects of changing the turbulent diffusivity in Section 5, we will describe how the diffusivity is changed. Similarly, in Section 6 we discuss the effects of turbulent pumping and explain how pumping is included in the mathematical theory.

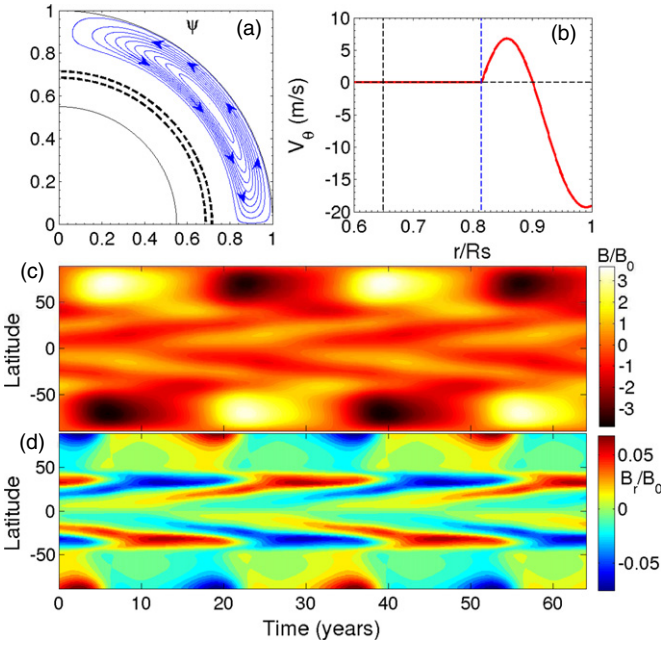

Figure 1. (a) Streamlines of the shallow meridional circulation with no flow underneath. (b) v_θ as a function of $r/R_\odot$ at the mid-latitude $\theta = 45°$. (c) Butterfly diagram, that is, the time-latitude plot of the toroidal field at the bottom of the convection zone ($r = 0.70\ R_\odot$). (d) Time-latitude plot of the radial field at the surface of the Sun. All the toroidal and radial fields are in units of B_0.

(A color version of this figure is available in the online journal.)

3. RESULTS WITH RADIALLY STACKED CELLS

First we consider when the meridional circulation has a return flow at the middle of the convection zone and there are no flows underneath it. We generate the meridional circulation by taking $\psi = \psi_u$ with ψ_u given by Equation (11). The upper part of Figure 1 shows the streamlines and the profile of v_θ as a function of r at the mid-latitude. The middle part of Figure 1 is

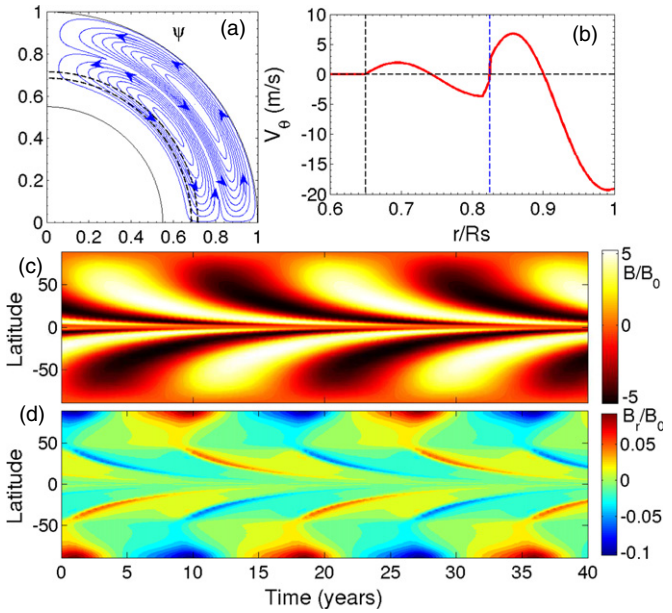

Figure 2. (a) Streamlines for two radially stacked cells of meridional circulation. Arrows show the direction of the flow. (b), (c), and (d) are the same plots as in Figure 1 for this meridional circulation.

(A color version of this figure is available in the online journal.)

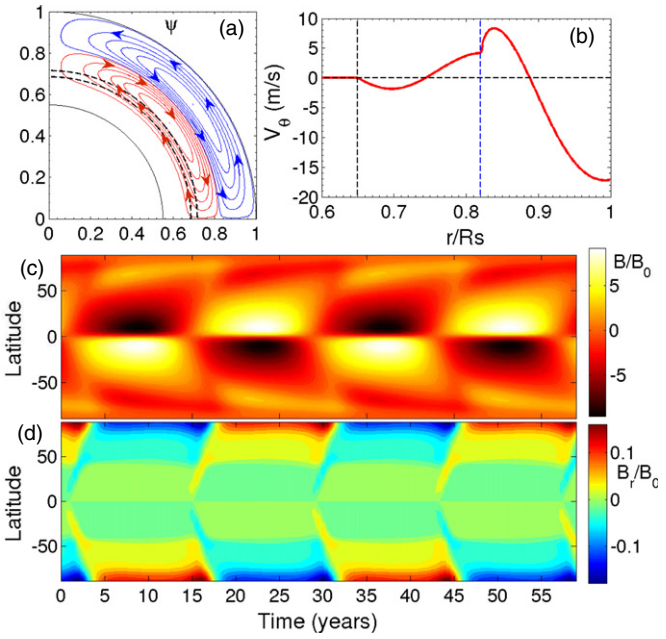

Figure 3. (a) Streamlines for two radially stacked cells of meridional circulation with circulations in the opposite sense. Arrows show the direction of the flow. (b), (c), and (d) are the same plots as in Figure 1 for this meridional circulation.

(A color version of this figure is available in the online journal.)

the "butterfly diagram," which is essentially a time-latitude plot of B at the bottom of the convection zone. The bottom part of the figure shows the radial field at the solar surface as function of time and latitude. In the butterfly diagram, we find that the belt of strong B propagates poleward rather than equatorward at the low latitudes, although there is a slight tendency of equatorward propagation at high latitudes. This result can be easily understood from the Parker–Yoshimura sign rule, which holds when there is no flow at the bottom of the convection zone. We have positive α in the northern hemisphere. Because $\partial\Omega/\partial r$ is positive in the low latitudes and negative in the high latitudes (see Figure 1 of Chatterjee et al. 2004, which shows the differential rotation we are using), the Parker–Yoshimura sign rule implies poleward propagation at low latitudes and equatorward propagation at high latitudes. In this case, we are unable to reproduce the solar behavior. It may be noted that Guerrero & de Gouveia Dal Pino (2008) obtained solar-like behavior with a meridional circulation similar to what we used by including equatorward latitudinal pumping at the bottom of the convection zone. However, there are some uncertainties about the nature of latitudinal pumping and the results of different simulations often do not match each other (Racine et al. 2011).

Next we consider the two-cell pattern given by Equations (10)–(12). For this case, Figure 2 provides plots similar to those shown in Figure 1 for the earlier case. There is an equatorward flow at the bottom of the convection zone, although there is a jump in v_θ between the cells. We find that the equatorward flow at the bottom forces an equatorward transport of B in accordance with what we see in the Sun. Looking at the lowest part of Figure 2, we also see that the polar field changes sign at the time of the sunspot maximum, in accordance with the observations. Thus, on using the two-cell pattern with an equatorward flow at the bottom of the convection zone, we can reproduce the equatorward migration of the sunspot zone as well as the correct phase relationship between the toroidal and poloidal fields. The butterfly diagram does start at a somewhat high latitude compared to what we see in the Sun. It is well known that the butterfly diagram can be confined more to lower latitudes by making the meridional circulation a more penetrating (Nandy & Choudhuri 2002) and playing with other parameters. We did not fine-tune the parameters to achieve this because we were focused on studying the qualitative behavior of the system under various kinds of meridional circulation. Note that in Figures 2(c) and (d) the maximum B at the bottom of the convection zone and the maximum B_r at the surface bear a ratio of about 100. It should be emphasized that this ratio corresponds to smoothed mean field values of B and B_r, which can have very different values inside flux concentrations (Choudhuri 2003).

We can avoid the jump in the value of v_θ seen in Figure 2(b) by using a two-cell meridional circulation in which ψ_l is replaced by $-\psi_l$. Because the flow at the bottom of the convection zone is poleward in this case, it also sheds light on the behavior of the dynamo with such a flow. Our results are shown in Figure 3. The butterfly diagram indicates poleward migration and the solar behavior is not reproduced in this case. The two-cell meridional circulation we used is very similar to what was used by Jouve & Brun (2007) in one of their cases (see their Figures 2 and 3). Our butterfly diagram is quite similar to theirs.

If we want to avoid a jump in v_θ and also having an equatorward flow at the bottom of the convection zone, then we need at least three cells of meridional circulation stacked one over the other in the radial direction. The Appendix provides the mathematical prescription for generating such a meridional circulation. Figure 4 presents the results. Because there is an equatorward flow at the bottom of the convection zone, we again find that the solar behavior is reproduced—in the sense of having a butterfly diagram showing equatorward migration, as well as the correct phase relationship between the toroidal and poloidal fields.

An important result for the flux transport dynamo with a single cell of meridional circulation is that the period of the dynamo decreases when the meridional circulation is made

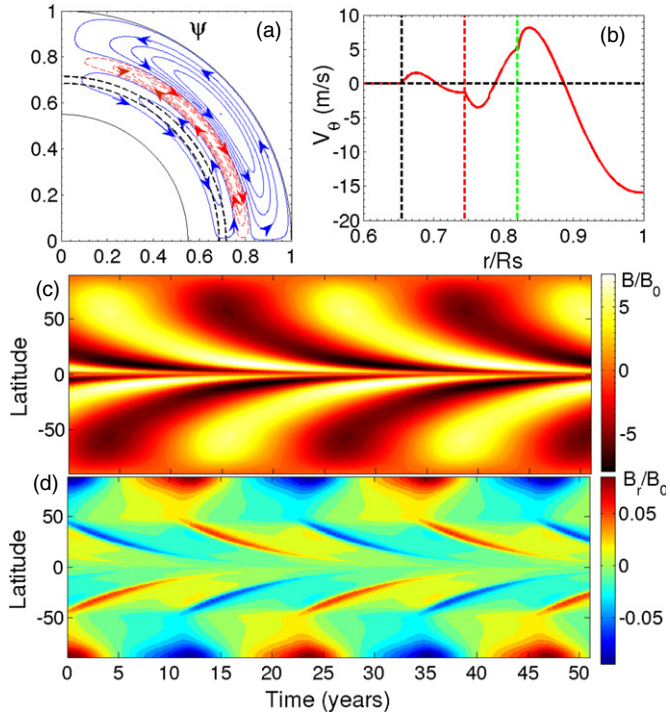

Figure 4. (a) Streamlines for three radially stacked cells of meridional circulation. Directions are shown by arrows. (b), (c), and (d) are the same plots as in Figure 1 for this meridional circulation.

(A color version of this figure is available in the online journal.)

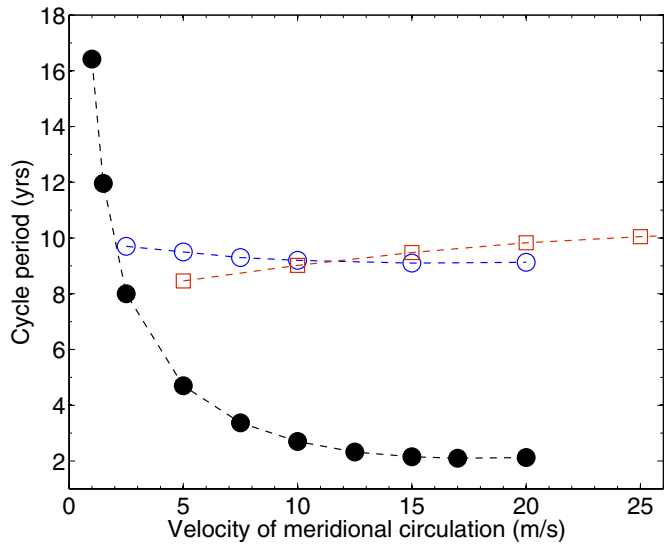

Figure 5. Variation of solar cycle period with the velocity amplitudes of the three different cells shown in Figure 4(a). Black filled circles show the variation of the cycle period with velocity amplitude of the lower cell, while keeping velocities of other cells constant. Similarly, blue circles show the variation of period with the velocity amplitude of the middle cell and red boxes for the upper cell.

(A color version of this figure is available in the online journal.)

faster (Dikpati & Charbonneau 1999; Karak 2010). To explore how the dynamo period depends on the flow velocity in the multi-cell situation, we carried out a study for the three cells presented in Figure 4. We carried out numerical experiments by varying the flow amplitude of one cell, while keeping the flows in the other two cells constant. Figure 5 shows how the dynamo period changes with the change of the flow speed in each of the three cells. It is clearly shown that the flow

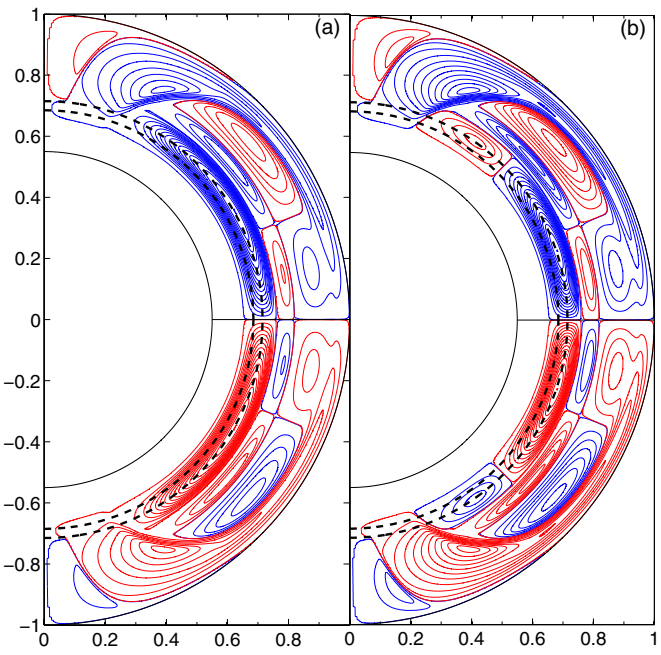

Figure 6. Streamlines for two complicated meridional circulation patterns. The blue contours imply counter-clockwise circulation, whereas the red contours imply clockwise circulation. The lowest cell in (a) extends from the equator to fairly high latitudes, whereas this cell in (b) only extends to mid-latitudes.

(A color version of this figure is available in the online journal.)

speeds in the upper two cells have a very minimal effect on the dynamo period. The flow speed in the lowermost cell is what determines the dynamo period and the period decreases with the increase in flow speed ($T \sim v_{0,l}^{-0.72}$). This result makes sense, as the flow in the lowermost cell causes the equatorward migration of B (giving solar-like butterfly diagram), and the period understandably becomes shorter when this flow is faster.

To sum up, as long as there is an equatorward flow at the bottom of the convection zone (the cases of Figures 2 and 4), we are able to get solar-like behavior of the dynamo even if there is a complicated multi-cell structure of the meridional circulation, the period being determined by the flow in the cell at the bottom of the convection zone. Thus, even with a return flow of the meridional circulation at a shallow depth, the flux transport dynamo model can be made to work in this situation. On the other hand, if there is no flow at the bottom of the convection zone (as shown in Figure 1) or if there is a poleward flow there (Figure 3), then the dynamo model fails to reproduce solar behavior. This conclusion was obtained by only considering multiple cells in the radial direction. We consider more complicated flows in the next section and show that our main conclusion still holds.

4. RESULTS WITH MORE COMPLICATED CELLS

We carried out some simulations with fairly complicated multi-cell meridional circulation which reinforced our main conclusion from the previous section: we can have solar-like dynamo solutions as long as there is an equatorward flow in low latitudes at the bottom of the convection zone. For the very complicated meridional circulation pattern shown in Figure 6(a), we present the results in Figure 7. The Appendix shows how this complicated flow was obtained from a suitable stream function. Because there is an equatorward flow in low latitudes at the bottom of the convection zone, we get

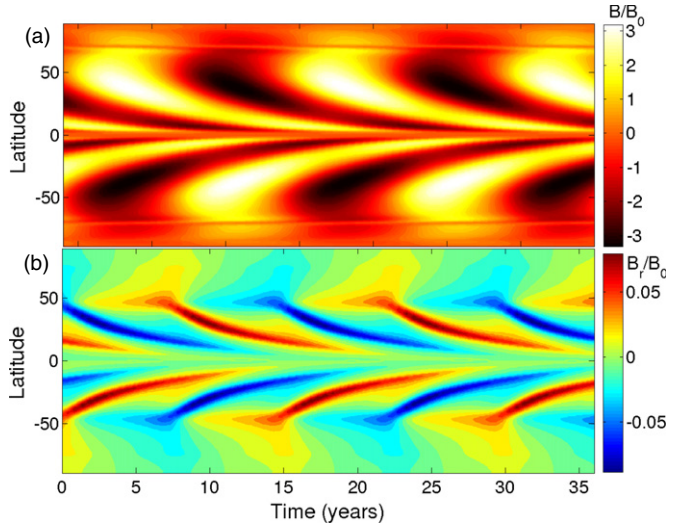

Figure 7. (a) and (b) are the same plots as (c) and (d) in Figure 1 for the meridional circulation given in Figure 6(a).
(A color version of this figure is available in the online journal.)

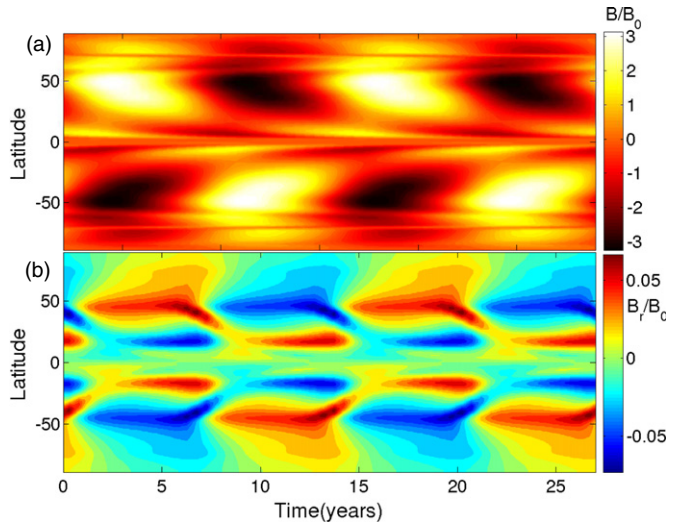

Figure 8. Same as Figure 7, for the meridional circulation given in Figure 6(b).
(A color version of this figure is available in the online journal.)

solar-like butterfly diagrams even with this flow. It should be noted that the lowermost cell in Figure 6(a) from the equator does not go all the way to the pole, but the cell ends at some high latitude. This cell has to extend sufficiently to reasonably high latitudes in order to give a solar-like butterfly diagram. If the cell does not extend beyond mid-latitudes, then we are unable to get very solar-like butterfly diagrams. In Figure 6(b) we show a meridional circulation with the lower cell not extending to high latitudes and the results are presented in Figure 8. We see that the butterfly diagram is much less realistic compared to the butterfly diagram presented in Figure 7. It is clear from Figures 7 and 8 that a solar-like butterfly diagram requires an equatorward flow at the bottom of the convection zone having a sufficient latitudinal extent from the equator to a reasonably high latitude.

5. RESULTS FOR LOW DIFFUSIVITY VERSUS HIGH DIFFUSIVITY

We have pointed out that the nature of the dynamo depends quite a bit on whether the turbulent diffusivity within the convection zone is assumed to be high or low (Jiang et al. 2007; Yeates et al. 2008; Hotta & Yokoyama 2010; Karak 2010; Karak & Choudhuri 2011). So far all the calculations in this paper have been carried out with a diffusivity on the higher side. With such diffusivity, the poloidal field generated near the surface by the Babcock–Leighton mechanism reaches the bottom of the convection zone primarily due to diffusion and this process is not affected by the presence of multiple cells. However, when the diffusivity is low, it is the meridional circulation that has to transport the poloidal field from the surface to the bottom of the convection zone and such transport becomes more complicated when there are multiple cells. Now we come to the question of whether our main conclusion in the previous two sections holds when the diffusivity is low. Following Chatterjee et al. (2004), we specify the diffusivity for the high diffusivity case in the following way:

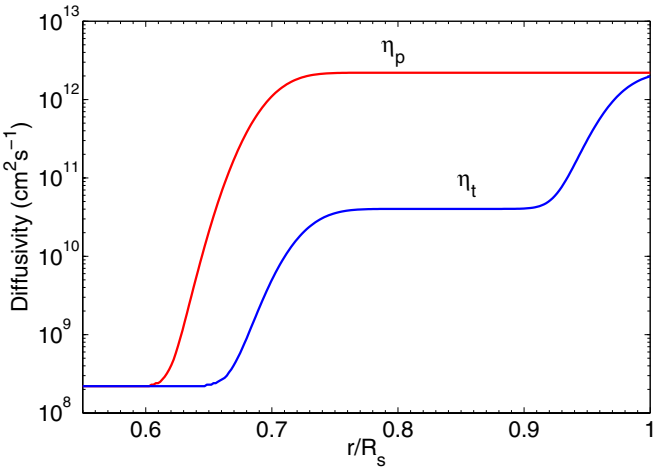

Figure 9. Plots of $\eta_p(r)$ and $\eta_t(r)$ as given by Equations (13) and (14). For the low diffusivity case we take $\eta_p = \eta_t$.
(A color version of this figure is available in the online journal.)

$$\eta_p(r) = \eta_{RZ} + \frac{\eta_{SCZ}}{2}\left[1 + \mathrm{erf}\left(\frac{r - 0.7\ R_\odot}{0.03\ R_\odot}\right)\right], \quad (13)$$

$$\eta_t(r) = \eta_{RZ} + \frac{\eta_{SCZ1}}{2}\left[1 + \mathrm{erf}\left(\frac{r - 0.725\ R_\odot}{0.03\ R_\odot}\right)\right] + \frac{\eta_{SCZ}}{2}\left[1 + \mathrm{erf}\left(\frac{r - 0.975\ R_\odot}{0.03\ R_\odot}\right)\right], \quad (14)$$

Here η_{RZ} is the diffusivity below the bottom of the convection zone, which is assumed to be small, whereas η_{SCZ} and η_{SCZ1} are the diffusivities of the poloidal and the toroidal components, respectively, within the body of the convection zone. Because the toroidal magnetic field is believed to be much stronger than the poloidal magnetic field, the diffusivity η_{SCZ1} of the toroidal field is assumed to be less than the diffusivity η_{SCZ} of the poloidal field. For the high diffusivity case (i.e., all the results presented in Sections 3 and 4), the values of the parameters for η_p are $\eta_{RZ} = 2.2 \times 10^8$ cm^2 s^{-1}, $\eta_{SCZ} = 2.2 \times 10^{12}$ cm^2 s^{-1}, and for η_t are $\eta_{SCZ1} = 4.0 \times 10^{10}$ cm^2 s^{-1}. Figure 9 shows these diffusivities as functions of r, which have been used in the calculations of Sections 3 and 4. Our aim in this section is to study the case when the diffusivity of the poloidal field is less. To achieve this, we take both η_p and η_t to be equal to η_t in the high diffusivity case, as given by Equation (14). This means

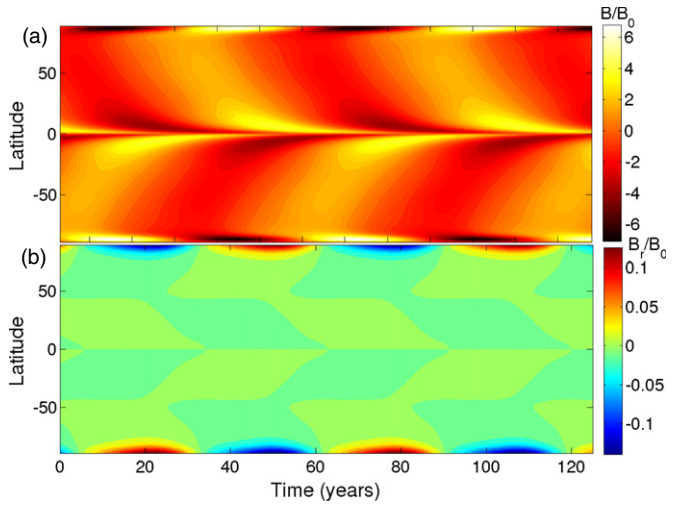

Figure 10. Same as Figure 7, for the case of the three radially stacked cells used in Figure 4, except that the diffusivity of the poloidal field is now lowered by making $\eta_p = \eta_t$.

(A color version of this figure is available in the online journal.)

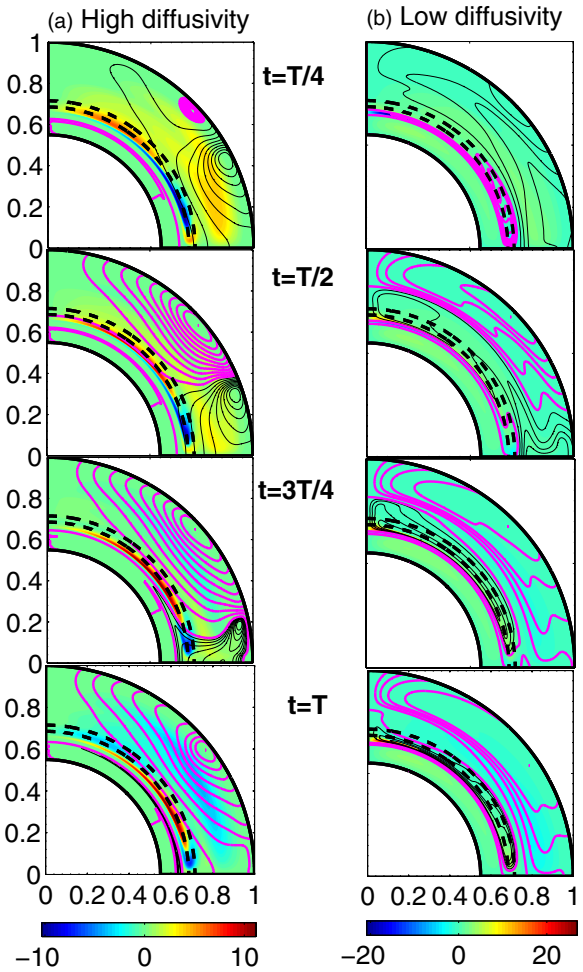

Figure 11. Poloidal field lines at four different stages of a solar cycle for the cases of (a) high diffusivity and (b) low diffusivity. The magenta and black colors indicate the clockwise and counter-clockwise sense of field lines, respectively. The background colors indicate the strength of the toroidal field.

(A color version of this figure is available in the online journal.)

that the diffusivity of the poloidal field within the main body of the convection zone is now reduced by a factor of more than 50 (from 2.2×10^{12} cm^2 s^{-1} to 4.0×10^{10} cm^2 s^{-1}) for the studies presented in this section.

To understand the effect of lowering the diffusivity, we carry on calculations for the case of three radially stacked cells (shown in Figure 4) by changing the diffusivity from the higher value to the lower value as mentioned previously. While reducing the diffusivity, we also reduce the strength of the α-coefficient as pointed out in Section 2. All the other parameters are kept unchanged. Figure 10 presents the results. Although we still find solar-like butterfly diagrams, the period becomes much larger on reducing the diffusivity. This is not surprising. When the diffusivity is low, the poloidal field generated by the Babcock–Leighton mechanism near the surface is transported to the bottom of the convection zone (where the toroidal field is generated from it) by the meridional circulation. If there is only one cell, then this is easily accomplished. However, when there are three radially stacked cells, the situation becomes much more complicated. The uppermost cell brings the poloidal field from the surface to its bottom. From there, the middle cell has to advect the poloidal field to its bottom. Finally, the lowermost cell takes the poloidal field to the bottom of the convection zone. In this process, the dynamo period increases. Figure 11 shows how the poloidal field lines evolve with the cycle with three radially stacked cells—both when the diffusivity is high (the case of Figure 4) and when it is low (the case of Figure 10). In the high diffusivity case, the poloidal field generated at the surface is transported downward to the bottom of the convection zone by diffusion. Thus, in this case, we find that the poloidal field lines are still not very different from what we find in the case of meridional circulation with one cell, as shown in Figure 4 of Jiang et al. (2007). However, when the diffusivity is low, the poloidal field is nearly frozen during a cycle and is advected by the meridional circulation. In a three-cell meridional circulation the poloidal field becomes very complicated, as shown in the right column of Figure 11.

It has been pointed out that, when we introduce fluctuations to model the irregularities of solar cycle, the dynamo models with high and low diffusivities behave completely differently (Jiang et al. 2007; Karak & Choudhuri 2011). In the high diffusivity model, the fluctuations diffuse all over the convection zone in timescales comparable to the dynamo period. On the other hand, fluctuations in the low diffusivity model remain frozen during the dynamo period. Jiang et al. (2007) explained how the observed correlation between the polar field during a sunspot minimum and the strength of the next cycle arises in the high diffusivity model. This correlation, which forms the basis of solar cycle prediction in the high diffusivity model, does not exist in the low diffusivity model. We now check if these results hold even when we have multiple cells of the meridional circulation. Choudhuri et al. (2007) identified the fluctuations in the Babcock–Leighton process as the main source of irregularity in the sunspot cycles. These fluctuations arise from the scatter in the tilt angles of sunspots caused by the effect of convective turbulence on rising flux tubes (Longcope & Choudhuri 2002). To model these fluctuations, we introduce stochastic fluctuations in α_0 appearing in Equation (5). We set

$$\alpha_0 \equiv \overline{\alpha_0}[1 \pm 0.75\sigma(\tau_{\rm cor})], \qquad (15)$$

where σ is a uniformly generated random number between 0 to 1 that changes value after a coherence time $\tau_{\rm cor} = 1$ month. This makes α_0 fluctuate randomly around its mean value $\overline{\alpha_0}$

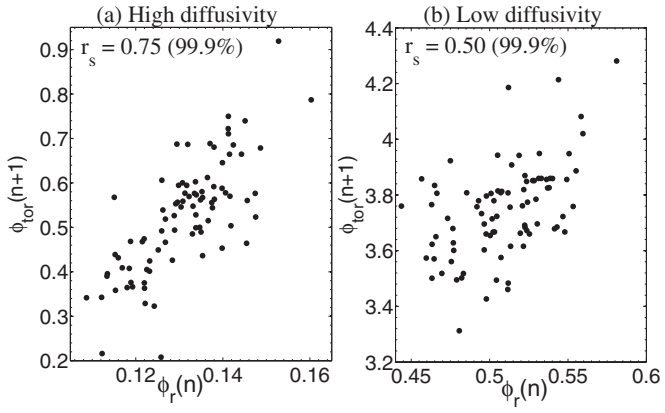

Figure 12. Correlation between peak polar flux strength at the end of the nth cycle and the peak toroidal flux strength of the $(n + 1)$th cycle for (a) high diffusivity and (b) low diffusivity cases.

with 75% amplitude of fluctuations. A simulation with such stochastic fluctuations in α in a traditional $\alpha\Omega$ dynamo model was first presented by Choudhuri (1992).

To study the correlation between the polar field and the strength of the next cycle, we consider the procedure of Yeates et al. (2008). We calculate the correlation between the peak of the surface radial flux ϕ_r at high latitudes of a cycle with that of the peak value of the deep-seated toroidal flux $\phi_{\rm tor}$ of the next cycle. We take ϕ_r as the flux of the radial field over the solar surface from latitude 70° to 89°, and $\phi_{\rm tor}$ as the flux of toroidal field over the region $r = 0.677\ R_\odot$ to $0.726\ R_\odot$ and latitude 10° to 45°. In the case of a one-cell meridional circulation (not presented in detail in this paper), we see a strong correlation between the high-latitude radial flux at the end of a cycle with the toroidal flux of the next cycle, with a correlation coefficient of 0.79, which is comparable to the result of Jiang et al. (2007, their Figure 5) and Yeates et al. (2008, their Figure 11(b)). Interestingly, for radially stacked three cells, we also get a strong correlation of 0.75 for the high diffusivity case. Figure 12 shows this result, along with the result for the low diffusivity case, which had a substantially poorer correlation. Thus, a multi-cell meridional circulation not only reproduces the regular periodic features of a simple flux transport dynamo model, it also reproduces some of the irregular features of the cycle if the diffusivity is high. The methodology for predicting the next cycle developed by Choudhuri et al. (2007) and Jiang et al. (2007) should work in approximately the same way in the high diffusivity model even when the meridional circulation has a complicated multi-cell structure.

6. THE EFFECT OF TURBULENT PUMPING

One possible mechanism for transporting magnetic fields across the solar convection zone that we have not yet mentioned is turbulent pumping. Many theoretical as well as numerical studies indicated that, in the strongly stratified solar convection zone, the magnetic fields can be pumped preferentially downward toward the base of the convection zone (Brandenburg et al. 1996; Tobias et al. 1998). Several magnetoconvection simulations have detected a downward pumping speed of a few meters per second in the solar convection zone (Ossendrijver et al. 2002; Käpylä et al. 2006; Racine et al. 2011). Guided by these studies, we now include the effect of turbulent pumping in our dynamo model by introducing the following downward

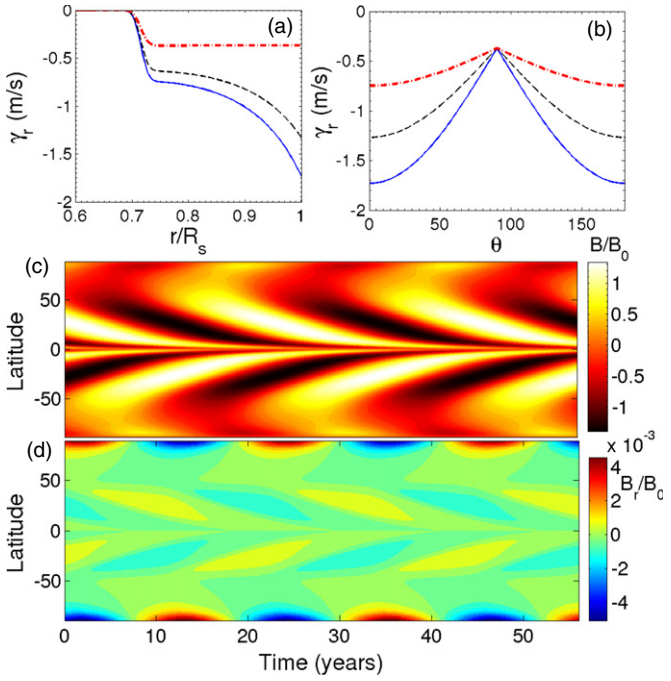

Figure 13. (a) Radial pumping γ_r as a function of radius at different colatitudes (θ). The solid (blue), dashed (black), and dash-dotted (red) lines correspond to $\theta = 90°, 45°$, and 0°, respectively. (b) γ_r as a function of θ at different radii. The solid (blue), dashed (black), and dash-dotted (red) lines correspond to $r = R_\odot$, $0.95\ R_\odot$, and $0.75\ R_\odot$, respectively. (c) and (d) are the same as (a) and (b) in Figure 10 with the radial pumping added.

(A color version of this figure is available in the online journal.)

pumping velocity:

$$\gamma_r = -0.1854\left[1+\mathrm{erf}\left(\frac{r-0.715\ R_\odot}{0.015\ R_\odot}\right)\right] \times\left[\exp\left(\frac{r-0.715\ R_\odot}{0.25\ R_\odot}\right)^2\cos\theta+1\right], \quad (16)$$

in units of m s^{-1}. The variations of γ_r as functions of radius and colatitude are shown in the upper part of Figure 13. Turbulent pumping appears as an advective term in the magnetic field equations. Therefore, in Equations (2) and (3), we add the extra term γ_r in the radial velocity (i.e., we take $v_r \equiv v_r + \gamma_r$). As in Karak & Nandy (2012), Kitchatinov & Olemskoy (2012), and Jiang et al. (2013), we first present results including only the radial pumping and not the latitudinal pumping.

Because the downward transport of the poloidal field by diffusion is reasonably efficient in the high diffusivity model, the effect of downward turbulent pumping is not very pronounced in this model. However, in the low diffusivity model, the poloidal field is advected by the meridional circulation in the absence of turbulent pumping and the addition of downward pumping can have quite dramatic effects. Karak & Nandy (2012) found that many of the differences between the high and the low diffusivity models disappear with the inclusion of downward turbulent pumping. Section 5 showed that the low diffusivity model with multi-cell meridional circulation gives results that do not match observations as closely as the results obtained with high diffusivity. Although the case of meridional circulation with three radially stacked cells, even with low diffusivity, produces reasonably good equatorward propagation of the toroidal field at low latitude, the solar cycle period becomes very long (see Figure 10). This calculation is

repeated for the low diffusivity case by including the downward pumping and the butterfly diagram is shown in the middle of Figure 13. The period becomes much shorter and the butterfly diagram looks quite similar to the butterfly diagram of Figure 4 in the high diffusivity case. Thus, even when multiple cells are present in the meridional circulation, the inclusion of downward turbulent pumping makes the results of the low diffusivity case quite similar to the results of the high diffusivity case.

A few magnetoconvection simulations (Ossendrijver et al. 2002; Käpylä et al. 2006; Racine et al. 2011) have detected a latitudinal turbulent pumping when rotation becomes important. However, while there is a general consensus about the radial downward pumping in the results of different groups, the results of latitudinal turbulent pumping are more uncertain and the physical origin is not easy to understand. In view of these uncertainties, we will not carry out a detailed study of the effects of latitudinal pumping in this paper. As we already mentioned, Guerrero & de Gouveia Dal Pino (2008) found that they could obtain solar-like solutions when including suitable equatorward latitudinal pumping, even when the return flow of the meridional circulation was at a shallow depth and there was no flow below it. We checked that we also get the same result when we include the latitudinal pumping used by Guerrero & de Gouveia Dal Pino (2008) in our model.

7. CONCLUSION

In the flux transport dynamo model, which has been very successful in modeling different aspects of the solar cycle, the meridional circulation of the Sun is a crucial ingredient. Currently, the major uncertainly in the flux transport dynamo model is our lack of knowledge about the nature of the meridional circulation in the deeper layers of the convection zone. Although two-dimensional models can never realistically treat magnetic buoyancy and the Babcock–Leighton mechanism, we do not believe that these uncertainties are so serious because different treatments of magnetic buoyancy and the Babcock–Leighton mechanism give qualitatively similar results (Nandy & Choudhuri 2001; Choudhuri et al. 2005). Because the meridional circulation arises out of a delicate imbalance between the centrifugal forcing and the thermal wind (Kitchatinov 2011), it is challenging to model it theoretically. Models of differential rotation based on a mean field treatment of turbulence give rise to a meridional circulation (Kitchatinov & Rüdiger 1995; Rempel 2005; Kitchatinov & Olemskoy 2011b). Magnetohydrodynamic (MHD) simulations of convection with the dynamo process also produce meridional circulations (Brown et al. 2010; Racine et al. 2011; Warnecke et al. 2013; Käpylä et al. 2013). In such simulations, the meridional circulation is often found to have several cells and vary rapidly with time. We are still far from having a definitive theoretical model of the Sun's meridional circulation.

Most of the flux transport dynamo models are based on the assumption of a single-cell meridional circulation having a return flow at the bottom of the convection zone. While support for such a return flow may have been missing, this assumption of a deeply penetrating single-cell meridional circulation was at least consistent with all the observational data available until about a couple of years ago. The equatorward propagation of the sunspot belt was indeed regarded as indicative of the meridional circulation flow velocity at the bottom of the convection zone (Hathaway et al. 2003). Only recently have there been claims that the meridional circulation may have a return flow at a much shallower depth (Hathaway 2012; Zhao et al. 2013). If these claims are corroborated by the independent investigations of other groups, then we will have to conclude that the assumption of a deep one-cell meridional circulation is not correct. Because this assumption was extensively used in most of the kinematic flux transport dynamo models, we now face a crucial question about whether this assumption is so essential that the flux transport dynamo models would not work without it or whether the flux transport dynamo models can still be made to work with a suitable modification of this assumption.

On the basis of our studies, we conclude that, in order for a flux transport dynamo to generate a solar-like butterfly diagram, we need an equatorward flow in low latitudes at the bottom of the convection zone. This flow is essential to overcome the Parker–Yoshimura sign rule and to advect the toroidal field generated in the tachocline in the equatorward direction. As long as there is such a flow, we find that the flux transport dynamo works even if the meridional circulation has a much more complicated structure than what has been assumed in previous models. If there is a return flow at a shallow depth and there are no flows underneath, then the flux transport dynamo will not work. If there is a poleward flow at the bottom of the convection zone, then also we do not get solar-like butterfly diagrams. However, underneath a shallow return flow, if we have multiple cells in such a way that there is an equatorward flow in low latitudes at the bottom of the convection zone, then the flux transport dynamo works without any serious problem. The assumption of such a multi-cell meridional circulation does not contradict any observational data available at the present time. MHD simulations also support the existence of a complicated multi-cell meridional circulation (Brown et al. 2010; Racine et al. 2011; Warnecke et al. 2013; Käpylä et al. 2013). With such a multi-cell meridional circulation we can retain all the attractive features of the flux transport dynamo model. The phase relation between the toroidal and poloidal fields is correctly reproduced. The observed correlation between the polar field during a sunspot minimum and the strength of the next cycle is also reproduced when the diffusivity is high, although a reduced diffusivity diminishes this correlation.

One of the important processes in the operation of the flux transport dynamo is the transport of the poloidal field generated near the surface by the Babcock–Leighton mechanism to the bottom of the convection zone where the differential rotation can act on it. We have taken higher diffusivity in the calculations presented in Sections 3 and 4 and we find that the poloidal field can diffuse from the surface to the bottom of the convection zone in a few years. A complicated multi-cell meridional circulation does not get in the way of this process. However, when the diffusivity is reduced, this transport has to be done by the meridional circulation. Interestingly, even in the case of low diffusivity with a multi-cell meridional circulation we are still able to get periodic solutions, although the poloidal field within the convection zone becomes very complicated and the cycle period is lengthened. A downward turbulent pumping helps to reduce the differences between the high and the low diffusivity models. There is no concensus at the present time about latitudinal pumping. However, we reproduce the result of Guerrero & de Gouveia Dal Pino (2008), that an equatorward pumping at the bottom of the convection zone can make a flux transport dynamo work even in the absence of a flow there. Because such equatorward pumping can have a profound effect on the dynamo, the nature of such pumping needs to be investigated thoroughly through magnetoconvection simulations.

To sum up, we do not think that the recent claims of an equatorward return flow at a shallow depth pose a threat to the

flux transport dynamo model. In particular, we see no reason to give up the attractive scenario that the strong toroidal field is produced and stored in stable regions of the tachocline, from which parts of this toroidal field break away to rise through the convection zone and produce sunspots. The crucial assumption necessary to make the flux transport dynamo work is an equatorward flow in low latitudes at the bottom of the convection zone. At present, we do not have observational data either supporting or contradicting it. Because the flux transport dynamo has been so successful in explaining so many aspects of the solar cycle, we expect this assumption of equatorward flow in low latitudes at the bottom of the convection zone to be correct and we hope that future observations will establish it. Only if future observations show this assumption to be incorrect, then a drastic revision of our current ideas about the solar dynamo will be needed at that time.

We thank an anonymous referee for valuable comments. This work was partially supported by the JC Bose Fellowship awarded to A.R.C. by the Department of Science and Technology, Government of India.

APPENDIX

STREAM FUNCTIONS FOR THE THREE-CELL AND MORE COMPLICATED MERIDIONAL CIRCULATION

To get three radially stacked cells shown in Figure 4(a), we take the stream function as

$$\psi = \psi_u + \psi_m + \psi_l. \quad \text{(A1)}$$

The stream function, which generates the upper cell, is given by

$$\psi_u = \psi_{0u}\left[1 - \mathrm{erf}\left(\frac{r - 0.87\,R_\odot}{1.5}\right)\right](r - R_{m,u})^{0.3} \times \sin\left[\frac{\pi(r - R_{m,u})}{(R_\odot - R_{m,u})}\right]\{1 - e^{-\beta_1\theta^\epsilon}\} \times \{1 - e^{\beta_2(\theta-\pi/2)}\}e^{-((r-r_0)/\Gamma)^2}, \quad \text{(A2)}$$

where the parameters have the following values: $\beta_1 = 3.5$, $\beta_2 = 3.3$, $r_0 = (R_\odot - R_b)/3.5$, $\epsilon = 2.0000001$, $\Gamma = 3.4 \times 10^8$ m, $R_{m,u} = 0.82\ R_\odot$. The stream function for middle cell is given by

$$\psi_m = \psi_{0m}\left[1 - \mathrm{erf}\left(\frac{r - 0.85R_{m,u}}{1.5}\right)\right](r - R_{m,l}) \times \sin\left[\frac{\pi(r - R_{m,l})}{(R_{m,u} - R_{m,l})}\right]\{1 - e^{-\beta_1\theta^\epsilon}\} \times \{1 - e^{\beta_2(\theta-\pi/2)}\}e^{-((r-r_0)/\Gamma)^2}, \quad \text{(A3)}$$

where the parameters have the following values: $\beta_1 = 1.9$, $\beta_2 = 1.7$, $r_0 = (R_\odot - R_b)/3.5$, $\Gamma = 3.4 \times 10^8$ m, $R_{m,l} = 0.75\ R_\odot$, $R_{m,u} = 0.82\ R_\odot$. Finally, the stream function, which generates lower cell, is

$$\psi_l = \psi_{0l}\left[1 - \mathrm{erf}\left(\frac{r - 0.75R_{m,l}}{0.8}\right)\right](r - R_p) \times \sin\left[\frac{\pi(r - R_p)}{(R_{m,l} - R_p)}\right]\{1 - e^{-\beta_1\theta^\epsilon}\} \times \{1 - e^{\beta_2(\theta-\pi/2)}\}e^{-((r-r_0)/\Gamma)^2}, \quad \text{(A4)}$$

where the parameters have the following values: $\beta_1 = 1.5$, $\beta_2 = 1.3$, $r_0 = (R_\odot - R_b)/3.5$, $\Gamma = 3.47 \times 10^8$ m, $R_p = 0.65\ R_\odot$, $R_{m,l} = 0.76\ R_\odot$. We choose ψ_{0u}/C, ψ_{0m}/C and ψ_{0l}/C in such a way that v_0 for upper cell, middle cell, and lower cell are around 17.0 m s^{-1}, 5.5 m s^{-1}, and 2.0 m s^{-1}, respectively.

In order to get the complicated meridional circulation as shown in Figure 6, we choose our stream function as given below

$$\psi = \psi_l + \psi_{lm} + \psi_m + \psi_u + \psi_{uc}, \quad \text{(A5)}$$

where,ψ_l, ψ_{lm}, ψ_m, ψ_u, and ψ_{uc} generate the lower cell, lower middle cells, middle cells, the complicated upper cell, and the upper corner cell, respectively. To give an idea about the kind of stream function we use in order to get a complicated cell, we write down the stream function ψ_u for the most complicated upper cell:

$$\psi_u = \psi_{0u}\left[1 + \mathrm{erf}\left(\frac{r - R_c}{0.02\ R_\odot}\right)\right]\sin\left[\frac{\pi(r - R_p)}{(R_\odot - R_p)}\right] \times (r - R_p)\{1 - e^{-\beta_1\theta^\epsilon}\}\{1 - e^{\beta_2(\theta-\pi/2)}\}e^{-((r-r_0)/\Gamma)^2} \quad \text{(A6)}$$

where

$$R_c = \frac{1}{2}\left[1 + \mathrm{erf}\left(\frac{\theta - \pi/24}{\pi/7}\right)\right] \times 0.95\ R_\odot,$$

and the parameters have the following values:

$\beta_1 = 0.45$, $\beta_2 = 1.3$, $r_0 = (R_\odot - R_b)/3.5$, $\Gamma = 3.1 \times 10^8$ m, $R_p = 0.65\ R_\odot$. Here do not write down the other stream functions, which are constructed along similar lines.

REFERENCES

Babcock, H. W. 1961, ApJ, 133, 572
Bonanno, A., Elstner, D., Belvedere, G., & Rüdiger, G. 2005, AN, 326, 170
Brandenburg, A., Jennings, R. L., Nordlund, A., et al. 1996, JFM, 306, 325
Braun, D. C., & Fan, Y. 1998, ApJL, 508, L105
Brown, B. P., Browning, M. K., Brun, A. S., Miesch, M. S., & Toomre, J. 2010, ApJ, 711, 424
Caligari, P., Moreno-Insertis, F., & Schussler, M. 1995, ApJ, 441, 886
Charbonneau, P. 2010, LRSP, 7, 3
Chatterjee, P., & Choudhuri, A. R. 2006, SoPh, 239, 29
Chatterjee, P., Nandy, D., & Choudhuri, A. R. 2004, A&A, 427, 1019
Choudhuri, A. R. 1989, SoPh, 123, 217
Choudhuri, A. R. 1992, A&A, 253, 277
Choudhuri, A. R. 1998, The Physics of Fluids and Plasmas: An Introduction for Astrophysicists (Cambridge: Cambridge Univ. Press)
Choudhuri, A. R. 2003, SoPh, 215, 31
Choudhuri, A. R. 2011, Prama, 77, 77
Choudhuri, A. R., Chatterjee, P., & Jiang, J. 2007, PhRvL, 98, 131103
Choudhuri, A. R., & Karak, B. B. 2009, RA&A, 9, 953
Choudhuri, A. R., & Karak, B. B. 2012, PhRvL, 109, 171103
Choudhuri, A. R., Nandy, D., & Chatterjee, P. 2005, A&A, 437, 703
Choudhuri, A. R., Schüssler, M., & Dikpati, M. 1995, A&A, 303, L29
Dasi-Espuig, M., Solanki, S. K., Krivova, N. A., Cameron, R., & Peñuela, T. 2010, A&A, 518, 7
Dikpati, M., & Charbonneau, P. 1999, ApJ, 518, 508
Dikpati, M., & Choudhuri, A. R. 1995, SoPh, 161, 9
Dikpati, M., de Toma, G., Gilman, P. A., Arge, C. N., & White, O. R. 2004, ApJ, 601, 1136
D'Silva, S., & Choudhuri, A. R. 1993, A&A, 272, 621
Durney, B. R. 1995, SoPh, 160, 213
Fan, Y., Fisher, G. H., & Deluca, E. E. 1993, ApJ, 405, 390
Giles, P. M., Duvall, T. L., Scherrer, P. H., & Bogart, R. S. 1997, Natur, 390, 52
Goel, A., & Choudhuri, A. R. 2009, RA&A, 9, 115
Guerrero, G., & de Gouveia Dal Pino, E. M. 2008, A&A, 485, 267
Hathaway, D. H. 2012, ApJ, 760, 84
Hathaway, D. H., Nandy, D., Wilson, R. M., & Reichmann, E. J. 2003, ApJ, 589, 665
Hotta, H., & Yokoyama, T. 2010, ApJL, 714, L308

Jiang, J., Cameron, R. H., Schmitt, D., & Isik, E. 2013, A&A, 553, 128
Jiang, J., Chatterjee, P., & Choudhuri, A. R. 2007, MNRAS, 381, 1527
Jouve, L., & Brun, A. S. 2007, A&A, 474, 239
Käpylä, P. J., Korpi, M. J., Ossendrijver, M., & Stix, M. 2006, A&A, 455, 401
Käpylä, P. J., Mantere, M. J., Cole, E., Warnecke, J., & Brandenburg, A. 2013, ApJ, 778, 41
Karak, B. B. 2010, ApJ, 724, 1021
Karak, B. B., & Choudhuri, A. R. 2011, MNRAS, 410, 1503
Karak, B. B., & Choudhuri, A. R. 2012, SoPh, 278, 137
Karak, B. B., & Choudhuri, A. R. 2013, RA&A, 13, 1339
Karak, B. B., & Nandy, D. 2012, ApJL, 761, L13
Kitchatinov, L. L. 2011, in Proc. of the First Asia-Pacific Solar Physics Meeting, ed. A. R. Choudhuri & D. Banerjee (Bengaluru: Astronomical Society of India), 71
Kitchatinov, L. L., & Olemskoy, S. V. 2011a, AstL, 37, 656
Kitchatinov, L. L., & Olemskoy, S. V. 2011b, MNRAS, 411, 1059
Kitchatinov, L. L., & Olemskoy, S. V. 2012, SoPh, 276, 3
Kitchatinov, L. L., & Rüdiger, G. 1995, A&A, 299, 446
Leighton, R. B. 1964, ApJ, 140, 1547
Longcope, D., & Choudhuri, A. R. 2002, SoPh, 205, 63
Miesch, M. S., Featherstone, N. A., Rempel, M., & Trampedach, R. 2012, ApJ, 757, 128
Moreno-Insertis, F. 1983, A&A, 122, 241
Moreno-Insertis, F., Schüssler, M., & Ferriz-Mas, A. 1992, A&A, 264, 686
Muñoz-Jaramillo, A., Dasi-Espuig, M., Balmaceda, L. A., & DeLuca, E. E. 2013, ApJL, 767, L25
Muñoz-Jaramillo, A., Nandy, D., Martens, P. C. H., & Yeates, A. R. 2010, ApJL, 720, L20
Nandy, D., & Choudhuri, A. R. 2001, ApJ, 551, 576
Nandy, D., & Choudhuri, A. R. 2002, Sci, 296, 1671
Ossendrijver, M., Stix, M., Brandenburg, A., & Rüdiger, G. 2002, ApJ, 394, 735
Parker, E. N. 1955, ApJ, 122, 293
Parker, E. N. 1975, ApJ, 198, 205
Pipin, V., & Kosovichev, A. G. 2013, ApJ, 776, 36
Racine, E., Charbonneau, P., Ghizaru, M., Bouchat, A., & Smolarkiewicz, P. K. 2011, ApJ, 735, 46
Rempel, M. 2005, ApJ, 622, 1320
Schad, A., Timmer, J., & Roth, M. 2013, ApJL, 778, L38
Tobias, S. M., Brummell, N. H., Clune, T. L., & Toomre, J. 1998, ApJL, 502, L177
Wang, Y.-M., Sheeley, N. R., & Nash, A. G. 1991, ApJ, 383, 431
Warnecke, J., Käpylä, P. J., Mantere, M. J., & Brandenburg, A. 2013, ApJ, 778, 141
Yeates, A. R., & Muñoz-Jaramillo, A. 2013, MNRAS, 436, 3366
Yeates, A. R., Nandy, D., & Mackay, D. H. 2008, ApJ, 673, 544
Yoshimura, H. 1975, ApJ, 201, 740
Zhao, J., Bogart, R. S., Kosovichev, A. G., Duvall, T. L., & Hartlep, T. 2013, ApJL, 774, L29